

Article

## Experimental Investigation on NO<sub>x</sub> Reduction by Primary Measures in Biomass Combustion: Straw, Peat, Sewage Sludge, Forest Residues and Wood Pellets

Ehsan Houshfar <sup>1,\*</sup>, Terese Løvås <sup>1</sup> and Øyvind Skreiberg <sup>2</sup>

<sup>1</sup> Department of Energy and Process Engineering, Norwegian University of Science and Technology (NTNU), Kolbjørn Hejes Vei 1B, Trondheim NO-7491, Norway; E-Mail: [terese.lovass@ntnu.no](mailto:terese.lovass@ntnu.no)

<sup>2</sup> SINTEF Energy Research, Trondheim NO-7465, Norway; E-Mail: [oyvind.skreiberg@sintef.no](mailto:oyvind.skreiberg@sintef.no)

\* Author to whom correspondence should be addressed; E-Mail: [ehsan.houshfar@ntnu.no](mailto:ehsan.houshfar@ntnu.no); Tel.: +47-73593896; Fax: +47-73593580.

Received: 6 December 2011; in revised form: 29 January 2012 / Accepted: 1 February 2012 /

Published: 8 February 2012

---

**Abstract:** An experimental investigation was carried out to study the NO<sub>x</sub> formation and reduction by primary measures for five types of biomass (straw, peat, sewage sludge, forest residues/Grot, and wood pellets) and their mixtures. To minimize the NO<sub>x</sub> level in biomass-fired boilers, combustion experiments were performed in a laboratory scale multifuel fixed grate reactor using staged air combustion. Flue gas was extracted to measure final levels of CO, CO<sub>2</sub>, C<sub>x</sub>H<sub>y</sub>, O<sub>2</sub>, NO, NO<sub>2</sub>, N<sub>2</sub>O, and other species. The fuel gas compositions between the first and second stage were also monitored. The experiments showed good combustion quality with very low concentrations of unburnt species in the flue gas. Under optimum conditions, a NO<sub>x</sub> reduction of 50–80% was achieved, where the highest reduction represents the case with the highest fuel-N content. The NO<sub>x</sub> emission levels were very sensitive to the primary excess air ratio and an optimum value for primary excess air ratio was seen at about 0.9. Conversion of fuel nitrogen to NO<sub>x</sub> showed great dependency on the initial fuel-N content, where the blend with the highest nitrogen content had lowest conversion rate. Between 1–25% of the fuel-N content is converted to NO<sub>x</sub> depending on the fuel blend and excess air ratio. Sewage sludge is suggested as a favorable fuel to be blended with straw. It resulted in a higher NO<sub>x</sub> reduction and low fuel-N conversion to NO<sub>x</sub>. Tops and branches did not show desirable NO<sub>x</sub> reduction and made the combustion also more unstable. N<sub>2</sub>O emissions were very low, typically below 5 ppm at 11% O<sub>2</sub> in the dry flue gas, except for mixtures with high nitrogen content, where values up to 20 ppm were observed. The presented results are part of a larger study on

problematic fuels, also considering ash content and corrosive compounds which have been discussed elsewhere.

**Keywords:** biomass mixtures; combustion;  $\text{NO}_x$ ; staged air; wood; straw; peat; sewage sludge

---

## 1. Introduction

According to the analysis carried out by the European Renewable Energy Council, the EU aims for a 100% renewable energy future by 2050, where biomass will potentially supply about 36% of the total European primary energy consumption, while the potential for many developing countries is higher since the resources are larger in such areas [1]. Biomass, with large resources around the World, which contains carbon in its structure, is almost a  $\text{CO}_2$ -neutral fuel. Combustion is the conventional way of extracting energy from biomass to produce heat, electricity or combined heat and power (CHP). Biomass can also be converted to synthetic natural gas or liquid fuels like methanol in order to be used in the transportation sector [2,3]. As a carbon- and nitrogen-containing fuel, combustion of biomass is nevertheless associated with emissions of harmful pollutants. Emissions from a biomass combustion process are normally divided into three groups [4,5]:

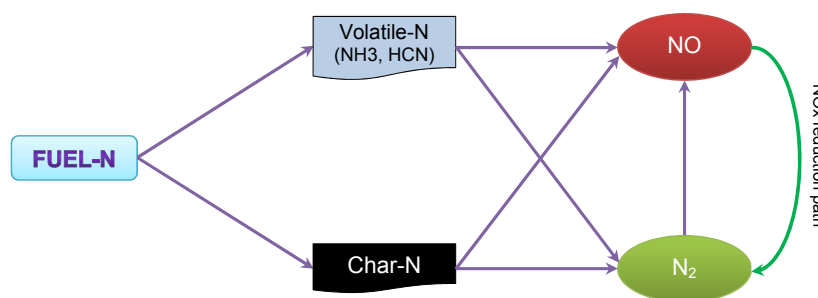
- (1) incomplete combustion products or unburnt species:  $\text{CO}$ ,  $\text{C}_x\text{H}_y$ , ...
- (2) complete combustion emissions:  $\text{CO}_2$ ,  $\text{H}_2\text{O}$ ,  $\text{NO}_x$ , ...
- (3) bottom ash and fly ash

In large industrial boilers, particles from incomplete combustion are generally low due to favorable combustion conditions [6]. However for each type of biomass, based on the source, characteristics and chemical composition, special care should be taken with certain emissions and residues as they can cause environmental problems [7]. For example sewage sludge needs consideration regarding the high ash content and the problems regarding ash removal from the reactor. Parallel studies on the same fuel batch show that straw needs care due to a low ash melting temperature and high alkali content which may cause damage to the tubes and walls via agglomeration, corrosion, deposition and fouling [8]. This was confirmed by others for varying types of reactors [9,10]. Furthermore, peat, sewage sludge and straw have all high nitrogen contents that results in a high  $\text{NO}_x$  emission level [11–14]. It is difficult to reduce all the mentioned pollutants simultaneously. There is e.g., a trade-off between  $\text{NO}_x$  emissions and unburnt hydrocarbons and carbon monoxide. Hence decreasing one may result in increases in another [15]. Furthermore nitrogen oxides ( $\text{NO}_x = \text{NO} + \text{NO}_2 + \text{NO}_3$ ) were classified as an indirect greenhouse gas in the Kyoto Protocol, by producing ozone via photochemical reactions in the atmosphere. The impact of  $\text{NO}_x$  emissions on global warming, acid rain, and formation of toxic chemicals should therefore be controlled.

Formation of  $\text{NO}_x$  occurs through four different processes: thermal  $\text{NO}_x$  (Zeldovich mechanism),  $\text{N}_2\text{O}$ -intermediate mechanism, prompt NO (Fenimore mechanism), and fuel-N conversion [11,16]. In solid fuels fired systems, fuel-NO accounts for more than 80% of the total  $\text{NO}_x$  and  $\text{NO}_x$  is mainly produced by conversion of volatile nitrogen-containing species such as  $\text{NH}_3$  and  $\text{HCN}$ , while

remaining char-N oxidation in the reactor bed accounts for a minor part of the total NO [11,17–22]. In addition, thermal NO<sub>x</sub> formation becomes important at temperatures above 1400 °C, which is far from the typical temperature range (800–1200 °C) of biomass combustion systems [16,23,24]. Experimental investigations are needed to characterize the release of nitrogen containing species from different solid biomass fuels to establish input for CFD modeling studies [25]. Figure 1 shows the conversion path for fuel-nitrogen in a conventional biomass combustion system.

**Figure 1.** Simple fuel nitrogen conversion path diagram.



The parameters that affect NO<sub>x</sub> formation and reduction potential are residence time, temperature, excess air ratio, fuel-N content, and mixing condition [26–29]. Temperature has the least influence on NO<sub>x</sub> formation as mentioned earlier due to relatively low temperature range of typical biomass combustion [26]. Note still that it is proved that reburning during oxy-combustion is more sensitive to temperature [30]. Also, NO<sub>x</sub> precursors, *i.e.*, ammonia and hydrogen cyanide, are very sensitive to temperature and the HCN/NH<sub>3</sub> ratio increases with increasing temperature [31–33].

Major technologies to reduce the NO<sub>x</sub> emissions, based on the fuel composition and combustion system are divided into two categories: primary measures and secondary measures [34]. Primary measures reduce the emissions within the combustion chamber or before fuel feeding, so the formation of NO<sub>x</sub> will be prevented as much as possible before the flue gases leave the reactor. These measures include staged air and staged fuel combustion, modification to the fuel composition by fuel blending, co-combustion, improvements to the combustion chamber, flue gas recirculation, fuel pretreatment, *etc.* [4,35–44]. *e.g.*, the use of biomass/coal cofiring has become more interesting due to the increased environmental performance of energy production from solid fuels at a moderate cost. Generally the sulfur content of biomass is lower than that of coal, so the SO<sub>x</sub> emissions from coal/biomass cofiring will be lowered since the sulfur content of the fuels blend has a lower level. Furthermore a reduction in NO<sub>x</sub> emissions is predicted in cofiring plants as the mixture has lower nitrogen content [45].

Secondary measures are used to remove the formed emissions from the flue gas, where selective catalytic reduction (SCR) and selective non-catalytic reduction (SNCR) are the most well-known secondary technologies and can reduce the NO<sub>x</sub> level up to 90%. However, the operation range and the overall economics of the plant should be considered before applying such costly methods [16,41,46,47]. Therefore, for small biomass combustion reactors, only primary reduction techniques are considered used in a feasible way. Air staging is most interesting in this respect due to its rather simple application and high NO<sub>x</sub> reduction potential. In an air staged scenario, the total air is divided and fed to the reactor in two stages. The majority of fuel-N is converted to HCN, NO and NH<sub>3</sub> in the first stage

where the primary excess air ratio is kept lower than, but close to, stoichiometric conditions. Thereafter, the remaining air is added to the reactor in the second stage. Ammonia is converted to  $\text{NH}_i$  and may form NO if fuel lean conditions exist in the second stage [48]. However, due to the under-stoichiometric condition in the second stage, HCN and  $\text{NH}_i$  radicals react with NO to form  $\text{N}_2$  responsible for the  $\text{NO}_x$  reduction [27]. Hence, keeping the primary excess air ratio at an optimum value is the key to minimize  $\text{NO}_x$  in staged air combustion.

Staged air combustion is widely applied in biomass combustion applications, both on the small scale and the large scale. Fuel staging follows a concept similar to air staging, but with addition of the fuel to the reactor in two stages. Some researchers tried to use a *combination* of the methods. Such combined staging (CS) was developed by Zabetta *et al.* [41] who used staged air, staged fuel and selective noncatalytic reduction (SNCR), and differs from other approaches since it pursues the reduction of  $\text{NO}_x$  via HCN as the key intermediate. The application of CS method is relative for the small burner or very fast engines where the residence time is too short to reach the maximum reduction from the simple staging technique. In addition, it needs more modification to the burner and is therefore costly. The reactor setup used in this study, however, has a long residence time which allows the maximum reduction via air staging.

In this work, experiments were performed in a fixed grate small scale multifuel reactor in order to investigate the  $\text{NO}_x$  emissions. The reactor has the possibility to facilitate both fuel and air staging, of which the latter has been the focus in this work. The fuels used in the present study are problematic fuels regarding ash related issues and corrosive content which make the combustion process complicated in large scale boilers. The ash related issues have been studied for the same batch of fuels and are presented and discussed elsewhere [8,49]. Furthermore, the selected biomasses cover a relatively broad range of nitrogen content and include straw, sewage sludge, peat, wood pellets, and tops and branches. Hence, the effect of initial fuel-N content on the conversion rate of nitrogen to  $\text{NO}_x$  is also investigated and discussed. Additional studies are needed on branches and tops due to a large resource potential in Northern Europe. Particularly it is necessary to investigate the emission levels from blends of fuels, and the effect this has on the expected optimum  $\text{NO}_x$  reduction potential by staged air combustion.

## 2. Materials and Methods

### 2.1. Sample Preparation

Five types of biomass and mixtures thereof were investigated to provide a wide basis for understanding emissions based on fuel characteristic. The selected fuels for this study were straw, sewage sludge, peat, virgin wood and forest residues (tops and branches) which had nitrogen content of 0.11–7.02 wt%. All fuels were pelletized to 6 mm diameter. Wood pellets and forest residues were obtained from Norwegian sources. Forest residues were collected from southern Norway, from stands with poor site quality. Peat was provided by Eidsiva Bioenergi AS. Sewage sludge and straw were provided through the SciToBiCom ERA-net by respectively Bioenergy2020+ (Austria) and DTU (Denmark). The wood pellet samples are hereby named WP, the forest residue samples GG (or Grot), and the Sewage Sludge samples SS, and so on. To prepare the fuel mixtures, the original fuels were

first grinded and then mixed and pelletized in a lab-scale pellet machine. Proximate and ultimate analyses were carried out both for the pure fuels and the mixtures. The results of the analyses are given in Table 1 and Table 2. ASTM E871, ASTM E872 and ASTM D1102 were used to measure moisture content, volatile matter and ash content of the fuels respectively and fixed carbon was obtained by difference to 100%.

**Table 1.** Ultimate analyses of the samples, wt% daf (dry, ash free).

	C	H	O	N	S	Cl
WP	51.4	6.1	42.4	0.11	0.05	0.02
GG	53.4	6.2	39.9	0.43	0.12	0.04
Straw	49.5	6.1	43.6	0.50	0.21	0.10
SS	48.9	7.4	34.6	7.02	2.07	0.10
Peat	56.0	6.1	35.0	2.60	0.34	0.02
WP + GG 5%	51.5	6.1	42.3	0.12	0.06	0.02
WP + GG 20%	51.7	6.1	41.9	0.17	0.07	0.02
WP + GG 50%	52.3	6.1	41.2	0.27	0.09	0.03
Straw + GG 20%	50.3	6.2	42.8	0.48	0.20	0.09
Straw + GG 50%	51.5	6.2	41.7	0.46	0.17	0.07
Straw + SS 5%	49.5	6.2	43.3	0.72	0.28	0.10
Straw + SS 10%	49.5	6.2	43.0	0.94	0.34	0.10
Straw + SS 20%	49.4	6.3	42.3	1.42	0.47	0.10
Straw + Peat 5%	49.8	6.1	43.3	0.58	0.22	0.10
Straw + Peat 20%	50.5	6.1	42.3	0.82	0.23	0.09
Straw + Peat 50%	52.2	6.1	40.0	1.39	0.27	0.06

**Table 2.** Proximate analyses of the samples (wt%, dry).

	VM	Fixed Carbon	Ash	Moisture (wet base)	HHV (MJ/kg)
WP	85.3	14.5	0.2	6.5	20.7
GG	77.0	20.7	2.3	9.6	21.8
Straw	78.7	16.4	4.9	11.7	19.9
SS	56.0	8.5	35.6	□	21.1
Peat	65.4	24.3	10.3	□	22.9
WP + GG 5%	84.6	15.0	0.4	14.4	20.8
WP + GG 20%	83.0	16.5	0.6	14.4	20.9
WP + GG 50%	80.7	18.0	1.3	11.8	21.2
Straw + GG 20%	77.9	17.7	4.4	13.8	20.4
Straw + GG 50%	77.5	18.9	3.6	11.8	20.9
Straw + SS 5%	77.6	16.1	6.3	12.8	20.0
Straw + SS 10%	76.6	15.5	7.9	15.4	20.0
Straw + SS 20%	73.6	14.6	11.8	9.4	20.0
Straw + Peat 5%	77.6	17.1	5.2	11.2	20.0
Straw + Peat 20%	77.1	17.1	5.9	14.4	20.3
Straw + Peat 50%	73.1	19.5	7.4	17.1	21.1

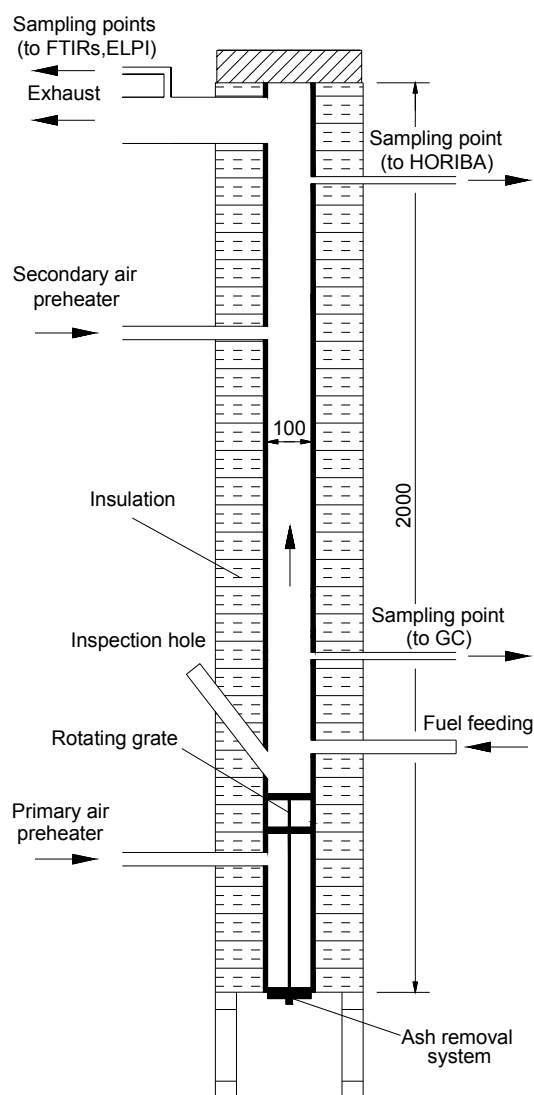
The mixtures were selected based on thermodynamic analyses to minimize the formation of corrosive components in the reactor and the results regarding corrosion abatement as presented and discussed in the earlier publications [8,49].

Small deviations (not presented) between the measured (Table 2) and calculated values exist for the composition of the mixture samples, which are probably due to the higher measurement uncertainties in the lowest measurement range [50]. This is discussed further in the Results section.

## 2.2. Experimental Setup

The combustion tests were carried out in SINTEF Energy Research's multifuel reactor, which is an electrically heated high temperature reactor. A schematic drawing is presented in Figure 2. The reactor has a ceramic inner tube with a diameter of 100 mm and a length of 2 m. The vertical tube consists of two 1 m long ceramic tubes connected with a ceramic socket. The ceramic tubes are made of non-porous and non-catalytic alumina.

**Figure 2.** Schematic of the multifuel reactor.

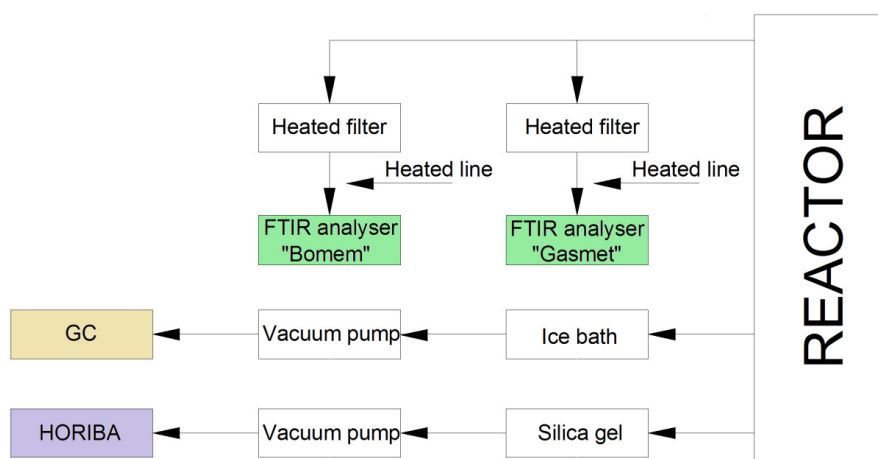


The reaction section, located above the grate, is 1.6 m long, while the section below the grate is 0.4 m long. The heating system is fitted inside the insulation shell and consists of four separate 0.5 m high heating zones of 4 kW each (16 kW in total) that enclose the ceramic tubes. The top and bottom of the reactor are insulated, but not heated, and both include detachable and insulated plates. The lower part of the multifuel reactor is the section containing the grate, which has two levels (10 cm apart), a primary grate and a final burnout grate and an ash collection system with an ash bin. The grate and the ash bin are both made of Inconel. The reactor setup thus combines two possible reduction technologies simultaneously, staged air and staged fuel combustion. The 2-level grate may give a possible fuel staging effect. The inlet air is preheated to the reactor temperature in external preheaters. The primary air is added under the grate (underfire air) and the secondary air is added above the grate (overfire air). The air flow is controlled by high precision digital mass flow controllers. The temperature inside the reactor is measured at several points. Furthermore, additional thermo-couples are used to control and protect the heating elements of the reactor from overheating. The preheating units have separate control systems. The temperatures are also monitored in the flue gas channel with four K-type thermocouples.

### 2.3. Gas Sampling

The flue gas composition, both at the reactor exit and in the primary zone, is continuously monitored. A schematic diagram of the sampling lines is shown in Figure 3.

**Figure 3.** Schematic diagram of the sampling lines.



For gas analysis in the primary zone, a Varian CP-4900 micro gas chromatograph (GC) was used. A stainless steel probe with an outside diameter (OD) of 10 mm and an inner diameter (ID) of 8 mm was used for the gas sampling. The sampled gas passed first through a tar, water and particle ice-cooled trap consisting of a steel container filled with glass wool and with a glass microfiber paper filter. The sampling gas flow was about 1 L/min. The GC was equipped with two Thermal Conductivity Detectors (TCDs) with a detection limit of 1 ppm, and double injectors, each connected to a separate column. The first column was a 10 m long PoraPLOT Q-type, with an inner diameter of 0.25 mm and a 10  $\mu$ m film thickness produced by Varian Inc., and uses helium as carrier gas. This column was used for the separation of CO<sub>2</sub>, CH<sub>4</sub>, C<sub>2</sub>H<sub>2</sub> + C<sub>2</sub>H<sub>4</sub> and C<sub>2</sub>H<sub>6</sub>. The second column was a 20 m long

CP-MolSieve 5A PLOT, with an inner diameter of 0.25 mm and a 30  $\mu\text{m}$  film thickness produced by Varian Inc., and used argon as carrier gas in order to be able to detect  $\text{H}_2$ . This column was able to quantify  $\text{H}_2$ ,  $\text{O}_2$ ,  $\text{N}_2$ ,  $\text{CH}_4$  and  $\text{CO}$ . The GC had a sampling time interval of approximately two minutes.

The exhaust gases were quantified online with a Gaset DX-4000 Fourier transform infrared (FTIR) spectrometer which was equipped with an integrated  $\text{ZrO}_2/\text{O}_2$ -analyzer, and a Mercury Cadmium Telluride (MCT) detector and had a maximum resolution of  $4\text{ cm}^{-1}$ . The sampling line and cell were heated to  $180\text{ }^\circ\text{C}$ . The cell volume was 0.4 L and the optical path length was 5 m. The FTIR was used to quantify  $\text{H}_2\text{O}$ ,  $\text{CO}_2$ ,  $\text{CO}$ ,  $\text{NO}$ ,  $\text{N}_2\text{O}$ ,  $\text{NO}_2$ ,  $\text{SO}_2$ ,  $\text{NH}_3$ ,  $\text{HCl}$ ,  $\text{HF}$ ,  $\text{CH}_4$ ,  $\text{C}_2\text{H}_6$ ,  $\text{C}_2\text{H}_4$ ,  $\text{C}_3\text{H}_8$ ,  $\text{C}_6\text{H}_{14}$ ,  $\text{CHOH}$ ,  $\text{HCN}$  and  $\text{O}_2$ . Extracted gases were passing through heated filters and heated lines, before reaching the FTIR. A stainless steel probe with an OD of 10 mm and an ID of 8 mm was used for sampling. The sampling position was located in the stack. The second FTIR spectrometer was a Bomem MB9100, which takes samples from a position near the first FTIR. This analyzer was used to measure all the species mentioned for Gaset in addition to  $\text{C}_4\text{H}_{10}$ . The analyses was done by a large cell heated to  $176\text{ }^\circ\text{C}$  with a  $1\text{ cm}^{-1}$  spectral resolution detector and with a measurement time interval of 80 s.

Flue gas samples were also extracted through a sampling point near the top of the reactor. An Inconel probe with 6 mm OD and 4 mm ID was used for sampling. The gas first passed through silica gel and was thereafter led to a HORIBA analyzer using a vacuum pump. The sampling rate was 0.4 L/min. The HORIBA PG-250 is a portable gas analyzer that can simultaneously measure up to five separate gas components. The HORIBA PG-250 uses non-dispersive infrared (NDIR) absorption to quantify  $\text{CO}$ ,  $\text{SO}_2$  and  $\text{CO}_2$ , cross-modulation ordinary pressure chemiluminescence to measure  $\text{NO}_x$ , and a galvanized Zr cell for  $\text{O}_2$  measurements. The sampling unit comprises a filter, a mist catcher, a pump, an electronic cooling unit, and an  $\text{NO}_2$  to  $\text{NO}$  converter.

Bottom ash collected in the ash bin was removed manually after each test. Unburnt carbon in the bottom ash was measured after each experiment by weighing the ash before and after exposing it to a temperature of  $550\text{ }^\circ\text{C}$  for a period of 20 h.

#### 2.4. Experimental Procedure

The experimental matrix is given in Table 3. The experiments were carried out with pellets of 6 mm diameter from five biomass fuels and mixes of these, all in air staging mode. Only isothermal experiments were performed with a reactor temperature of  $850\text{ }^\circ\text{C}$ . The total excess air ratio was about 1.6, and the primary excess air ratio was about 0.8, however due to small variations in the fuel feeding rate, a range of excess air ratios was obtained during stable period of the experiments.

The fuel pellets were fed automatically from a fuel container located over a water-cooled piston. The perfectly sealed piston transported the fuel into the reactor and the pellets fell on the upper grate, thereafter the piston quickly returned to its starting position and the process was repeated. The feeding frequency was set to approximately 6–7 seconds, based on the fuel density and pellets size distribution, to ensure a fuel feeding rate of about 400 g/h.

**Table 3.** The experimental matrix.

Experiment No.	Fuel 1	Fuel 2	Fuel 2 in the mixture (wt%)
1	Wood Pellet	-	-
2	Wood Pellet	Grot	5%
3	Wood Pellet	Grot	20%
4	Wood Pellet	Grot	50%
5	Grot	-	-
6	Straw	Grot	20%
7	Straw	Grot	50%
8	Straw	Sewage Sludge	5%
9	Straw	Sewage Sludge	10%
10	Straw	Sewage Sludge	20%
11	Straw	Peat	5%
12	Straw	Peat	20%
13	Straw	Peat	50%

The pellets were mainly combusted on the upper (primary) grate. Then the pellets were gradually moved to a slot leading to the second (final burnout) grate by means of rotating blades. Each grate had two rotating blades rotating slowly around and completing a circle in around three minutes. Final burnout took place on the lower grate before the ash is moved to the ash bin. At the bottom of the ash bin another rotating blade moved the ash into an ash tube. The gas residence time between the grate levels was in the range of 1–2 s. and the total residence time of fuel gases in the reactor was 25–50 s, due to the very low flow velocity (0.03–0.07 m/s).

### 3. Results and Discussion

The carbon and hydrogen balance as a function of total excess air ratio for one of the experiments (mixture of straw 50% + peat 50%) is shown in Figure 4. As shown, the deviation between the measured and calculated values is in the range of  $\pm 2\%$ , so the experimental measurements are reliable with low uncertainty. The same trend was seen for all the other experiments (results not presented).

Combustion quality was also checked for all experiments with regard to unburnt species. The concentration of CO and  $C_xH_y$  (as ppm at 11%  $O_2$  in the dry flue gas) is shown in Figure 5 for the experiment with “straw 80% + grot 20%”. Due to the relatively long residence times (25–50 s), good mixing and high temperatures, the amounts of CO and unburnt hydrocarbons were very low. For the other mixtures CO and  $C_xH_y$  were below 50 ppm and 5 ppm at 11%  $O_2$  in dry flue gas, respectively. Hence, in all experiments the combustion can be considered complete under the given conditions. This is important to ensure that measurements of fuel-N originating  $NO_x$  are representative for what may be expected under normal and efficient running conditions.

**Figure 4.** Carbon and hydrogen balance check: CO<sub>2</sub> and H<sub>2</sub>O concentration and measured deviation for the experiment with “Straw 50% + Peat 50%”.

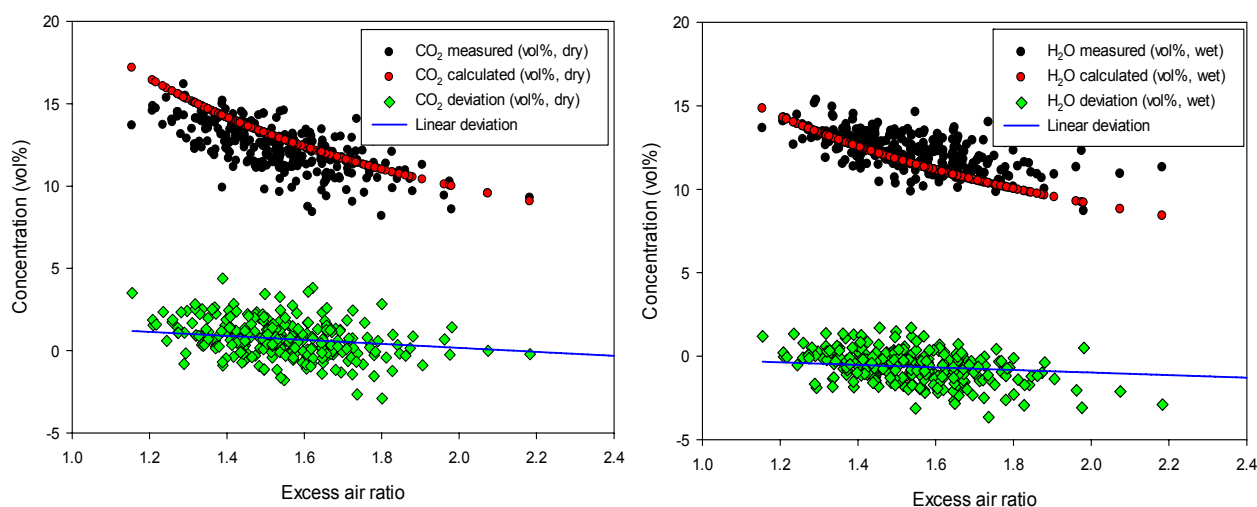
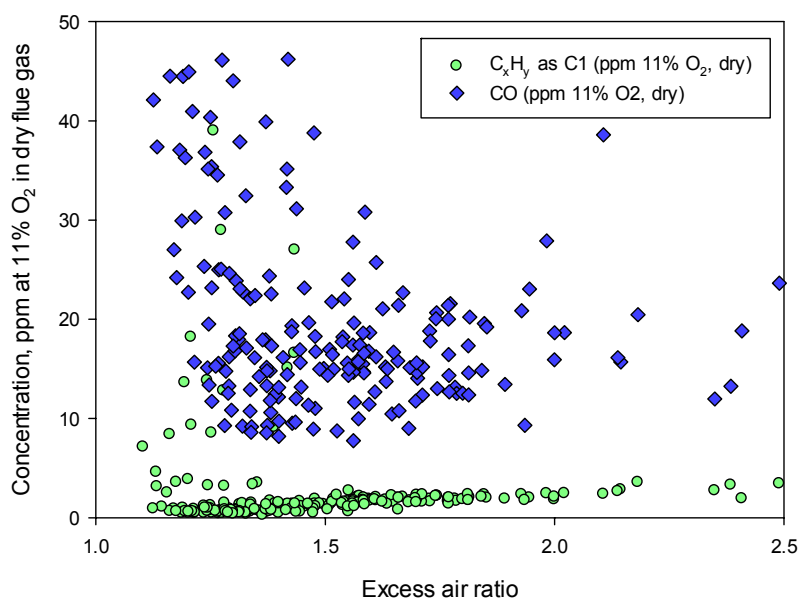


**Figure 5.** Unburnt gases (CO and C<sub>x</sub>H<sub>y</sub>): concentration as ppm at 11% O<sub>2</sub> in dry flue gas for the experiment with “Straw 80% + Grot 20%”.



### 3.1. NO<sub>x</sub> Reduction in Air Staged Combustion

The experiments revealed the NO<sub>x</sub> reduction potential with staged air combustion. The primary excess air ratio was the key influencing factor for NO<sub>x</sub> reduction in the set of experiments, where the results were especially relevant for a grate-furnace. In Figures 6–9 the effect of primary excess air ratio for different mixtures of straw, peat, sewage sludge, forest residues and wood pellets are compared.

**Figure 6.** Influence of the primary excess air ratio on the  $\text{NO}_x$  emissions from “straw + peat” mixtures for air staging (temperature: 850 °C,  $\text{NO}_x$  as ppm in dry flue gas at 11%  $\text{O}_2$ ).

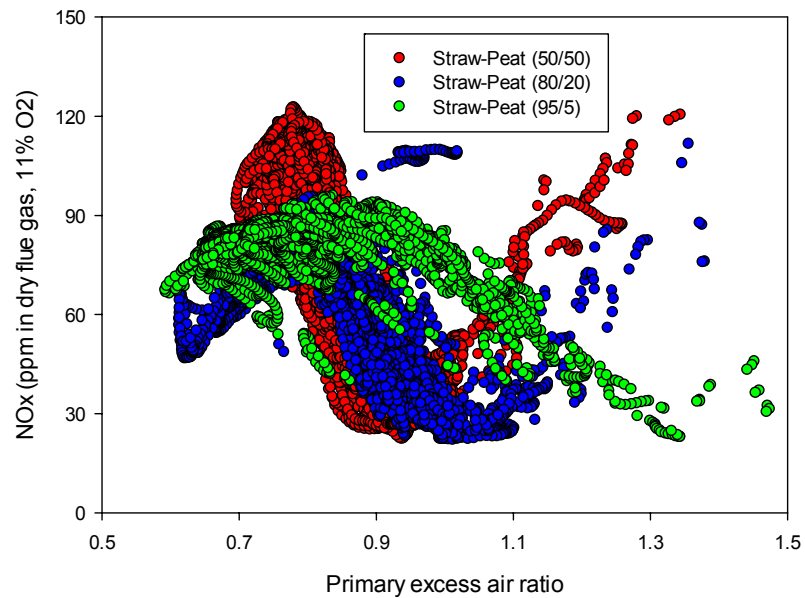


**Figure 7.** Influence of the primary excess air ratio on the  $\text{NO}_x$  emissions from “straw + sewage sludge” mixtures for air staging (temperature: 850 °C,  $\text{NO}_x$  as ppm in dry flue gas at 11%  $\text{O}_2$ ).

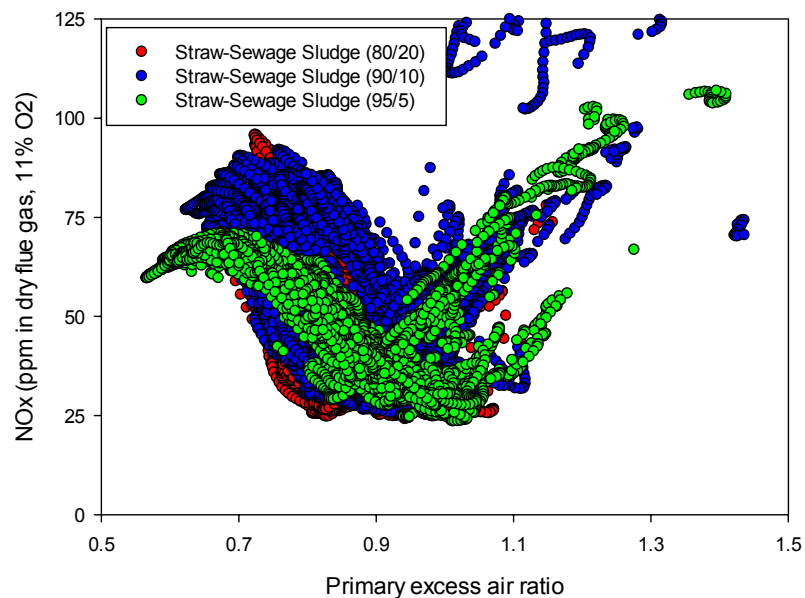


**Figure 8.** Influence of the primary excess air ratio on the  $\text{NO}_x$  emissions from “straw + tops and branches” mixtures for air staging at a temperature of 850 °C.

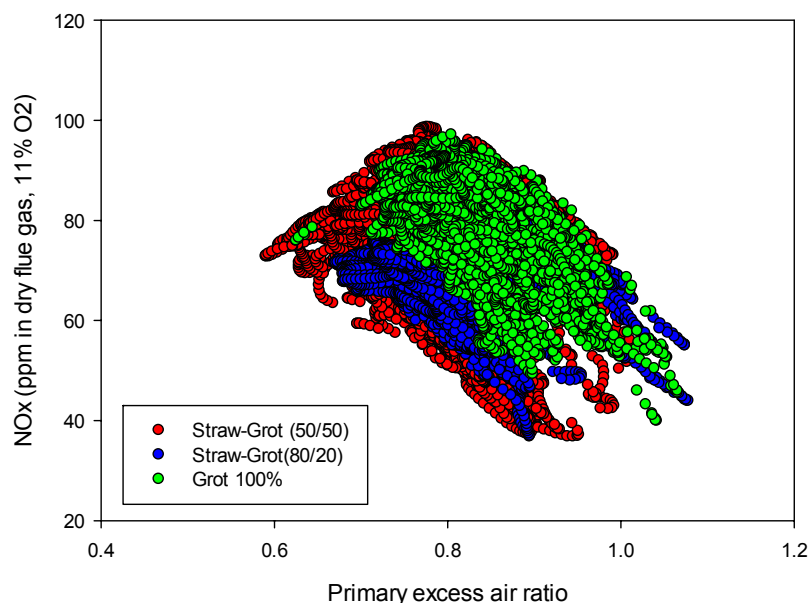
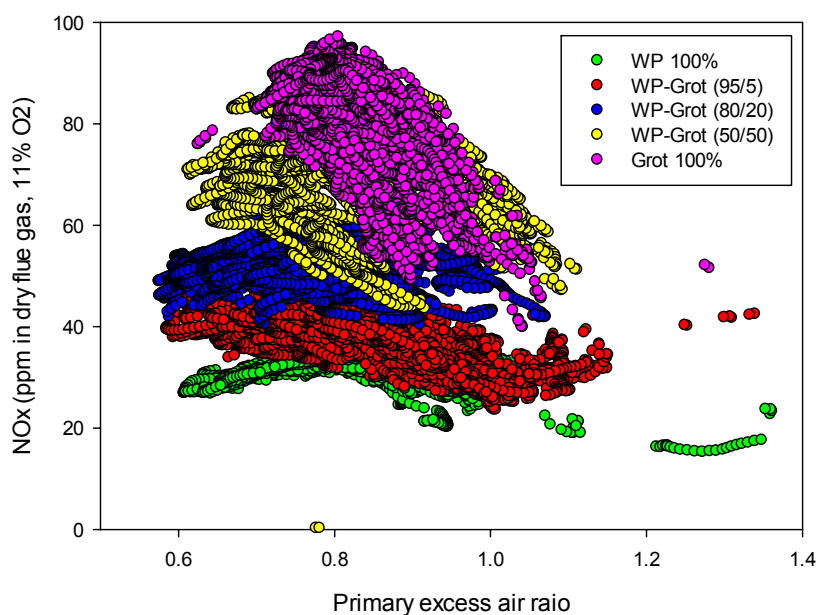


**Figure 9.** Influence of the primary excess air ratio on the  $\text{NO}_x$  emissions from “wood pellet + tops and branches” mixtures at a temperature of 850 °C.



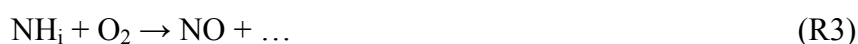
The  $\text{NO}_x$  level was clearly reduced when the primary excess air ratio increased up to about 1. An optimum reduction was found for almost all the experiments at a primary excess air ratio close to 0.9. The optimum primary excess air ratio for combustion of “straw 95% + peat 5%” was however found around 1.3 as seen in Figure 6 which is high for typical values of optimum primary excess. This needs some more clarifications. In this experiment, because of a high share of straw in the mixture, the ash melting temperature for the fuel blend was low, and 5 wt% peat did not improve the ash melting behavior of straw. Hence, during the running of the reactor, sintering happened on the grate, which caused the air slots on the grates to be filled with melted ash. In this case the actual “available oxygen”

for the fuel in the reactor was clearly lower than the amount of air which was fed to the reactor. Therefore the real primary excess air ratio for the case “straw 95% + peat 5%” may be regarded as a value closer to the other experiments, *i.e.*, 0.9–0.95. Similar problems were also observed for “straw 80% + peat 20%”, which explains that the optimum point is shifted toward an excess air ratio of 1, by the same interpretation. This issue is of course related to the design of the reactor. However, as it is not uncommon with such fuel grates in a conventional combustor, low ash melting properties for certain fuels [9] should be considered when designing for optimum combustion of biomass.

The reduction in NO<sub>x</sub> level for the staged air experiments was found to start from a primary excess air ratio of about 0.7 and continue to the highest reduction on the excess air ratio of about 0.9. However, further increase in the excess air ratio increased again the NO<sub>x</sub> emissions. This can be explained by the staged combustion effect. In the first stage, primary air was added for devolatilization of the volatile fraction of the fuel, which forms a fuel gas composed of mainly CO, H<sub>2</sub>, C<sub>x</sub>H<sub>y</sub>, H<sub>2</sub>O, CO<sub>2</sub> and N<sub>2</sub>. In addition, supplying less air than stoichiometric condition in a range of 0.7–0.9 causes the volatile-N fraction to form nitrogen containing NO<sub>x</sub> precursors. Therefore, small amounts of NH<sub>3</sub>, HCN, HOCN and NO will be produced depending on the fuel nitrogen content, temperature and other operating conditions. In the second stage, sufficient air is fed to the reactor to ensure final burnout of emissions from incomplete combustion, *e.g.*, CO, C<sub>x</sub>H<sub>y</sub>. Adding the remaining air in the second stage creates the path for NO reduction, where NO<sub>x</sub> act as an oxidant agent for the other N-containing species and also products of incomplete combustion (NH<sub>2</sub>, NH<sub>3</sub>, CO, CH<sub>4</sub>, ...) in reactions such as:



In the regions where the injected primary air is very low, the oxygen will not be sufficient for NO formation and just NH<sub>i</sub> and HCN will appear in the first stage from the fuel nitrogen. Following that, in the second stage, the remaining secondary air provides more than enough O<sub>2</sub>, so the formation of NO from its precursors' oxidation will be elevated following the reaction:



In contrast, when the primary excess air increases above 1, excess oxygen in the first stage will cause the oxidation of all pyrolysis gases. Therefore much more NO will appear while no sufficient NH<sub>i</sub> exists for the second stage to minimize the NO emissions via the reduction path, reaction (1), resulting in a raised NO emission level in the flue gas.

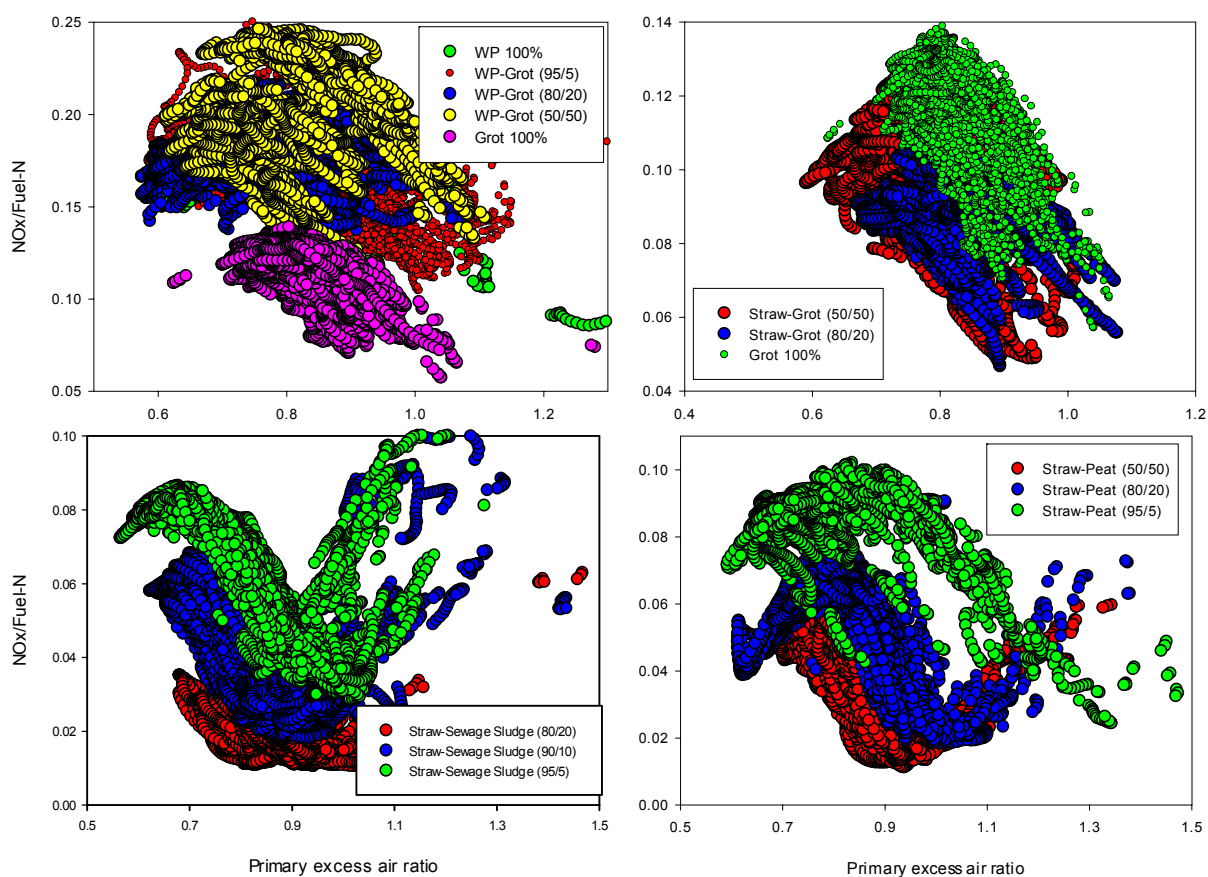
The results of staged air combustion of wood pellet and forest residues mixtures are presented in Figure 9. For better comparison, the results from pure wood and 100% grot are also included in the graph. Grot shows higher NO<sub>x</sub> emissions which are due to its higher nitrogen content. The NO<sub>x</sub> reduction is also limited to 40–50% for WP at the optimum excess air ratio. It is important to note that the NO<sub>x</sub> reduction potential depends greatly on the fuel nitrogen content. A reduction of 50–80% is observed for the experiments where 80% reduction corresponds to the experiment with highest nitrogen content in the fuel blend, *i.e.*, “straw 50% + peat 50%”. This will be discussed further below.

### 3.2. Effect of Fuel-N Content on N-Conversion: $NO_x$

For comparison purposes and to evaluate the conversion of the fuel nitrogen to  $NO_x$ , the ratio  $NO_x/\text{Fuel-N}$  is generally used. This ratio is obtained by dividing the total amount of nitrogen that exists in the measured  $NO_x$  in the flue gas by the nitrogen content of the biomass input. The major part of  $NO_x$  was by far composed of NO for the set of experiments at the given conditions.

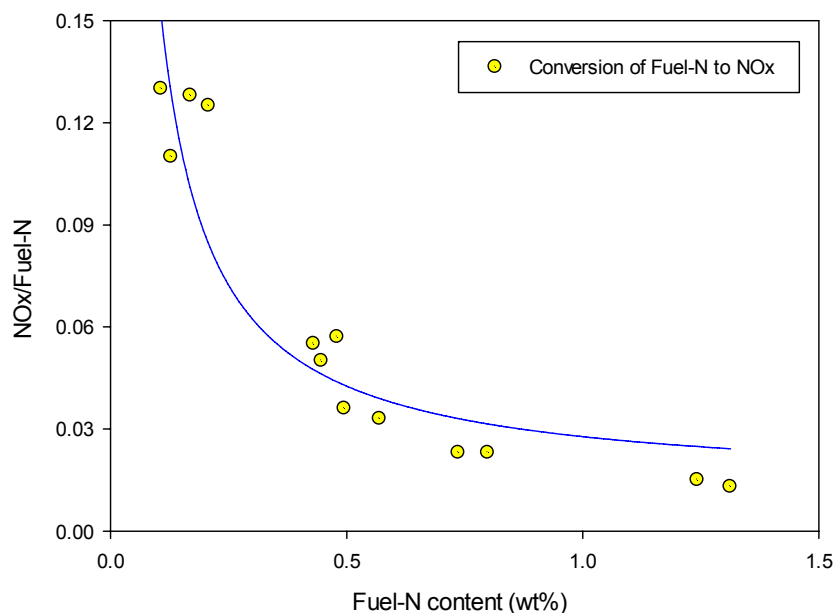
$NO_x/\text{Fuel-N}$  results are presented in Figure 10 for the fuels and mixtures at different stoichiometric ratios. It is shown that the nitrogen conversion level depends greatly on the fuel nitrogen content. The mixtures with wood pellets, which have the lowest fuel-N content, revealed high conversion of nitrogen to  $NO_x$ , while mixtures with peat converted considerably less nitrogen to  $NO_x$ .

**Figure 10.** Fuel-N conversion and the effect of fuel-N content.



The plot in Figure 11 summarizes the conversion rate of fuel nitrogen to  $NO_x$  with respect to the investigated fuels nitrogen content. The results are derived from the combustion at the optimum condition, *i.e.*, primary excess air ratio of 0.9–0.95. Therefore this graph shows the minimum potential fuel-N conversion to  $NO_x$  in the grate reactor. However, the trend for other excess air ratios is the same, where the fuels and blends with high nitrogen content typically convert only 2% of the fuel-N to  $NO_x$ .

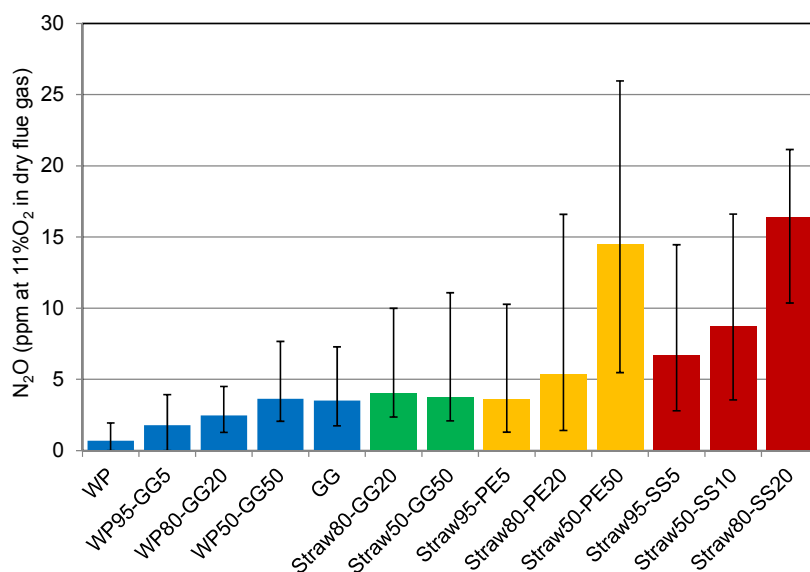
**Figure 11.** Influence of fuel-N content on the conversion to NO<sub>x</sub>.



3.3. Effect of Fuel-N Content on N-Conversion: N<sub>2</sub>O

The N<sub>2</sub>O concentration in the flue gas is shown in Figure 12. Nitrous oxide emissions are typically low, below 5 ppm at 11% O<sub>2</sub> in the dry flue gas. However, it should be noticed that the N<sub>2</sub>O level for a number of experiments with high nitrogen content in the fuel was up to 25 ppm. The N<sub>2</sub>O concentration increased with primary excess air ratio. Unburnt species such as CO and CH<sub>4</sub> that are reductive agents for NO<sub>x</sub>, as discussed earlier, have proven to promote the fuel-N conversion to N<sub>2</sub>O in high excess air ratios [51]. Therefore, the conditions which are in general favorable for NO<sub>x</sub> reduction result in more N<sub>2</sub>O formation.

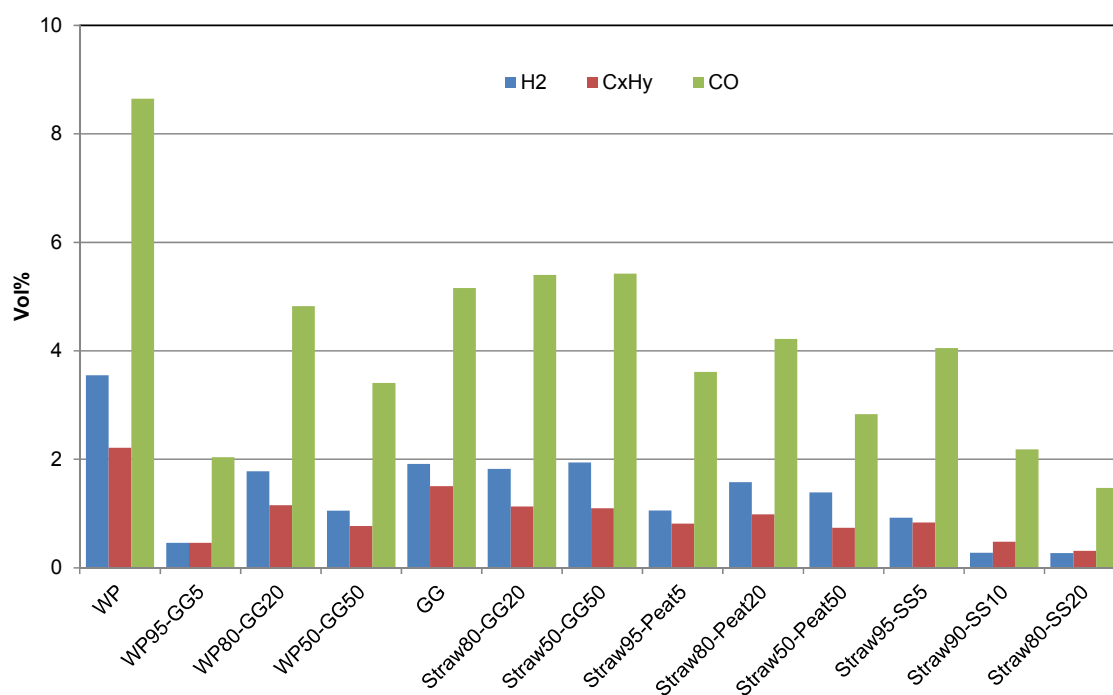
**Figure 12.** Effect of the primary excess air ratio on the N<sub>2</sub>O emissions at a temperature of 850 °C.



### 3.4. Effect of Fuel Type on $NO_x$

Figure 13 presents the yields of the main unburnt gases in the primary zone.  $CO$ ,  $H_2$  and  $CH_4$  were measured by a GC. The proximate analysis of the fuels reveals that the five original fuels are very different from each other, especially regarding ash content and volatile matters. The volatile matter (VM) contents of the selected original fuels ranged from around 56 to 85 wt% (dry basis) with ash contents from 0.2 to about 36 wt%. Wood pellets have the lowest ash and highest VM, while the highest ash and lowest VM belongs to sewage sludge. However, the volatile content of GG and straw are quite close to each other, even though straw has two times higher ash content. Obviously, the volatiles are very important for the nitrogen release and especially for the share of char or volatile nitrogen content, which finally affect the  $NO_x$  reduction path. Ash elemental composition should also be considered in a fuel type discussion, since elements such as calcium can act as catalyst to reduce nitrogen oxides [52]. Addition of fuels with higher volatile content would result in higher  $NO_x$  reduction, since the availability of radical species necessary for  $NO$  reduction is higher in the combustion zone. This is related to the reaction mechanism which is explained in the previous section, reactions R1-R3.

**Figure 13.** Level of main unburnt species in the primary zone for different fuels and mixtures.



On the other hand, release of char nitrogen is affected by particles residence time, size of pellets and the amount of inorganic elements, where the latter is being determined by the fuel type [11]. Due to the special design of our reactor (two level grate), the potential effect of volatile species interaction with the char matrix should also be considered as a potential significant factor. Straw mixtures with 20% GG, peat and SS give the following results: blending with GG gives the highest VM and the lowest Ca in the mixture. Contrary, the mixture of straw with SS has the lowest VM and the highest Ca. There is a competition between the explained mechanism for nitrogen release and reduction. Although GG has

higher volatile content and release a higher amount of volatile species according to Figure 13, the minimum  $\text{NO}_x$  emission and  $\text{NO}_x/\text{Fuel-N}$  for Straw + GG20 is significantly higher than for the other two blends. The  $\text{NO}_x$  reduction potential was also in the lowest range for this GG mixture, around 50%. Hence, it is suggested that GG is not a good selection to be blended with straw in order to reduce fuel- $\text{NO}_x$  emissions. However, peat and SS showed a higher  $\text{NO}_x$  reduction (75–80%) with a minimum  $\text{NO}_x$  level of about 20–25 ppm at 11%  $\text{O}_2$  in dry flue gas. Figure 13 shows lower volatiles amounts from SS mixtures compared to peat mixtures, so it seems that the effect of the reduction reaction R2 has been minimal in this case compared to other mechanisms. Finally, sewage sludge gives the lowest fuel-N conversion to  $\text{NO}_x$  compared to the other mixtures which makes this fuel a proper blend for straw combustion. It is suggested that SS addition to straw leads to increased mineral matters on the grate, hence resulting in catalytic activities of ash elements leading to  $\text{NO}_x$  reduction by CO or  $\text{CH}_4$ . However, further investigations are required to quantify the effect of the mentioned mechanism solely.

#### 4. Conclusions

The present study demonstrated that air-staging can be effectively used in a grate combustion reactor in order to reduce the  $\text{NO}_x$  emissions. Furthermore, staged air combustion for different biomass fuels and in particular mixtures of the selected fuels were investigated. Staged air combustion reduced the  $\text{NO}_x$  emissions significantly. However, the reduction level depended on the stoichiometric ratio of the first stage. An optimum primary excess air ratio of about 0.9 was found for the reactor in the primary zone (fuel rich condition). However, low ash melting characteristics of some of the fuels, particularly straw, caused this value to be somewhat higher due to sintering on the fuel grate. The  $\text{NO}_x$  level was reduced with 50–80% based on the fuel type. Mixtures with high nitrogen content showed higher reduction potential while wood pellets with the lowest nitrogen content showed less reduction. The unburnt species' concentration ( $\text{CO}$  and  $\text{C}_x\text{H}_y$ ) was very low in all cases due to the good combustion quality. Regarding fuel-N conversion to  $\text{NO}_x$ , this depends on the nitrogen content of the biomass. The fuels with lower nitrogen content showed a higher conversion of fuel-N to  $\text{NO}_x$ , while a blend of peat and sewage sludge, which had high fuel-N content, only converted about 2% of the fuel-N, the rest being converted directly to  $\text{N}_2$ , and a minor part remained in ash. SS, having low VM and high ash content, is suggested as a favorable fuel to be blended with straw, showing high  $\text{NO}_x$  reduction and low fuel-N conversion. GG, however, with high VM and low ash content, did not show desirable  $\text{NO}_x$  reduction and also made the combustion more unstable. The reduction potential for GG and SS mixtures was about 50% and 80%, respectively.

#### Acknowledgments

The authors wish to acknowledge the financial support from the Research Council of Norway and a number of industrial partners through the project KRAV (“Enabling small scale biomass CHP in Norway”). We also thank Bioenergy2020+ and DTU for providing fuels through SciToBiCom ERA-net Bioenergy project.

## References

1. Zervos, A.; Lins, C.; Muth, J. *RE-Thinking 2050*; European Renewable Energy Council, Renewable Energy House: Brussels, Belgium, 2010.
2. Borgwardt, R.H. Methanol production from biomass and natural gas as transportation fuel. *Ind. Eng. Chem. Res.* **1998**, *37*, 3760–3767.
3. Jurascik, M.; Sues, A.; Ptasiński, K.J. Exergetic evaluation and improvement of biomass-to-synthetic natural gas conversion. *Energy Environ. Sci.* **2009**, *2*, 791–801.
4. Nussbaumer, T. Combustion and co-combustion of biomass: Fundamentals, technologies, and primary measures for emission reduction. *Energy Fuels* **2003**, *17*, 1510–1521.
5. Khan, A.A.; de Jong, W.; Jansens, P.J.; Spliethoff, H. Biomass combustion in fluidized bed boilers: Potential problems and remedies. *Fuel Process. Technol.* **2009**, *90*, 21–50.
6. Johansson, L.S.; Tullin, C.; Leckner, B.; Sjövall, P. Particle emissions from biomass combustion in small combustors. *Biomass Bioenergy* **2003**, *25*, 435–446.
7. Obernberger, I.; Brunner, T.; Bärnthaler, G. Chemical properties of solid biofuels—significance and impact. *Biomass Bioenergy* **2006**, *30*, 973–982.
8. Khalil, R.A.; Houshfar, E.; Musinguzi, W.; Becidan, M.; Skreiberg, Ø.; Goile, F.; Løvås, T.; Sørum, L. Experimental investigation on corrosion abatement in straw combustion by fuel-mixing. *Energy Fuels* **2011**, *25*, 2687–2695.
9. Nielsen, H.P.; Frandsen, F.J.; Dam-Johansen, K. Lab-scale investigations of high-temperature corrosion phenomena in straw-fired boilers. *Energy Fuels* **1999**, *13*, 1114–1121.
10. Thy, P.; Jenkins, B.M.; Williams, R.B.; Leshner, C.E.; Bakker, R.R. Bed agglomeration in fluidized combustor fueled by wood and rice straw blends. *Fuel Process. Technol.* **2010**, *91*, 1464–1485.
11. Glarborg, P.; Jensen, A.D.; Johnsson, J.E. Fuel nitrogen conversion in solid fuel fired systems. *Prog. Energy Combust. Sci.* **2003**, *29*, 89–113.
12. Ren, Q.; Zhao, C.; Duan, L.; Chen, X. NO formation during agricultural straw combustion. *Bioresour. Technol.* **2011**, *102*, 7211–7217.
13. Giuntoli, J.; de Jong, W.; Verkooijen, A.H.M.; Piotrowska, P.; Zevenhoven, M.; Hupa, M. Combustion characteristics of biomass residues and biowastes: Fate of fuel nitrogen. *Energy Fuels* **2010**, *24*, 5309–5319.
14. Aho, M. Pyrolysis and combustion of peat and wood as single particles and as a layer. *J. Anal. Appl. Pyrolysis* **1987**, *11*, 149–162.
15. Eskilsson, D.; Rönnbäck, M.; Samuelsson, J.; Tullin, C. Optimisation of efficiency and emissions in pellet burners. *Biomass Bioenergy* **2004**, *27*, 541–546.
16. Mahmoudi, S.; Baeyens, J.; Seville, J.P.K. NO<sub>x</sub> formation and selective non-catalytic reduction (SNCR) in a fluidized bed combustor of biomass. *Biomass Bioenergy* **2010**, *34*, 1393–1409.
17. Permchart, W.; Kouprianov, V.I. Emission performance and combustion efficiency of a conical fluidized-bed combustor firing various biomass fuels. *Bioresour. Technol.* **2004**, *92*, 83–91.
18. Qian, F.P.; Chyang, C.S.; Huang, K.S.; Tso, J. Combustion and NO emission of high nitrogen content biomass in a pilot-scale vortexing fluidized bed combustor. *Bioresour. Technol.* **2011**, *102*, 1892–1898.

19. Winter, F.; Wartha, C.; Hofbauer, H. NO and N<sub>2</sub>O formation during the combustion of wood, straw, malt waste and peat. *Bioresour. Technol.* **1999**, *70*, 39–49.
20. Aho, M.J.; Hämäläinen, J.P.; Tummavuori, J.L. Importance of solid fuel properties to nitrogen oxide formation through HCN and NH<sub>3</sub> in small particle combustion. *Combust. Flame* **1993**, *95*, 22–30.
21. Hämäläinen, J.P.; Aho, M.J.; Tummavuori, J.L. Formation of nitrogen oxides from fuel-N through HCN and NH<sub>3</sub>: a model-compound study. *Fuel* **1994**, *73*, 1894–1898.
22. Hämäläinen, J.P.; Aho, M.J. Effect of fuel composition on the conversion of volatile solid fuel-N to N<sub>2</sub>O and NO. *Fuel* **1995**, *74*, 1922–1924.
23. Salzmann, R.; Nussbaumer, T. Fuel staging for NO<sub>x</sub> reduction in biomass combustion: Experiments and modeling. *Energy Fuels* **2001**, *15*, 575–582.
24. Lopes, M.H.; Gulyurtlu, I.; Cabrita, I. Control of pollutants during FBC combustion of sewage sludge. *Ind. Eng. Chem. Res.* **2004**, *43*, 5540–5547.
25. Stubenberger, G.; Scharler, R.; Zahirovic, S.; Obernberger, I. Experimental investigation of nitrogen species release from different solid biomass fuels as a basis for release models. *Fuel* **2008**, *87*, 793–806.
26. Houshfar, E.; Skreiberg, Ø.; Løvås, T.; Todorović, D.; Sørum, L. Effect of excess air ratio and temperature on NO<sub>x</sub> emission from grate combustion of biomass in the staged air combustion scenario. *Energy Fuels* **2011**, *25*, 4643–4654.
27. Skreiberg, Ø.; Glarborg, P.; Jensen, A.D.; Dam-Johansen, K. Kinetic NO<sub>x</sub> modelling and experimental results from single wood particle combustion. *Fuel* **1997**, *76*, 671–682.
28. Kolb, T.; Jansohn, P.; Leuckel, W. Reduction of NO<sub>x</sub> emission in turbulent combustion by fuel-staging/effects of mixing and stoichiometry in the reduction zone. *Symp. (Int.) Combust.* **1989**, *22*, 1193–1203.
29. Jenkins, B.M.; Baxter, L.L.; Miles, T.R. Combustion properties of biomass. *Fuel Process. Technol.* **1998**, *54*, 17–46.
30. Normann, F.; Andersson, K.; Johnsson, F.; Leckner, B. NO<sub>x</sub> reburning in oxy-fuel combustion: A comparison between solid and gaseous fuels. *Int. J. Greenhouse Gas Control* **2011**, *5*, S120–S126.
31. Hansson, K.-M.; Samuelsson, J.; Tullin, C.; Åmand, L.-E. Formation of HNCO, HCN, and NH<sub>3</sub> from the pyrolysis of bark and nitrogen-containing model compounds. *Combust. Flame* **2004**, *137*, 265–277.
32. Ren, Q.; Zhao, C.; Wu, X.; Liang, C.; Chen, X.; Shen, J.; Wang, Z. Formation of NO<sub>x</sub> precursors during wheat straw pyrolysis and gasification with O<sub>2</sub> and CO<sub>2</sub>. *Fuel* **2010**, *89*, 1064–1069.
33. Becidan, M.; Skreiberg, Ø.; Hustad, J.E. NO<sub>x</sub> and N<sub>2</sub>O precursors (NH<sub>3</sub> and HCN) in pyrolysis of biomass residues. *Energy Fuels* **2007**, *21*, 1173–1180.
34. Berndes, G.; Baxter, L.; Coombes, P.; Delcarte, J.; Evald, A.; Hartmann, H.; Jansen, M.; Koppejan, J.; Livingston, W.; van Loo, S.; *et al.* *The Handbook of Biomass Combustion and Co-Firing*; Earthscan: London, UK, 2008.

35. Padinger, R.; Leckner, B.; Åmand, L.-E.; Thunman, H.; Ghirelli, F.; Nussbaumer, T.; Good, J.; Hassler, P.; Salzmann, R.; Winter, F.; *et al.* Reduction of Nitrogen Oxide Emissions from Wood Chip Grate Furnaces — Final Report for the EU-JOULE III Project JOR3-CT96-0059. In *Proceedings of 1st World Conference on Biomass for Energy and Industry*, Sevilla, Spain, 5–9 June 2000; Kyritsis, S., Beenackers, A.A.A.M., Helm, P., Grassi, A., Chiaramonti, D., Eds.; James & James (Science Publishers) Ltd.: Sevilla, Spain, 2000; pp. 1457–1463.
36. Padinger, R. NO<sub>x</sub> Reduction of Biomass Combustion by Optimized Combustion Chamber Design and Combustion Control. In *Progress in Thermochemical Biomass Conversion*; Blackwell Science Ltd.: Hoboken, NJ, USA, 2008; pp. 918–928.
37. Kicherer, A.; Spliethoff, H.; Maier, H.; Hein, K.R.G. The effect of different reburning fuels on NO<sub>x</sub>-reduction. *Fuel* **1994**, *73*, 1443–1446.
38. Kristensen, P.G.; Glarborg, P.; Dam-Johansen, K. Nitrogen chemistry during burnout in fuel-staged combustion. *Combust. Flame* **1996**, *107*, 211–222.
39. Weissinger, A.; Obernberger, I.; Scharler, R. NO<sub>x</sub> Reduction in Biomass Grate Furnaces by Primary Measures — Evaluation by Means of Lab-Scale Experiments and Chemical Kinetic Simulation Compared with Experimental Results and CFD Calculations of Pilot-Scale Plants. In *Proceedings of 6th European Conference on Industrial Furnaces and Boilers*, Estoril, Portugal, 2–5 April 2002.
40. Svoboda, K.; Pohořelý, M.; Hartman, M. Effects of operating conditions and dusty fuel on the NO<sub>x</sub>, N<sub>2</sub>O, and CO emissions in PFB co-combustion of coal and wood. *Energy Fuels* **2003**, *17*, 1091–1099.
41. Zabetta, E.C.; Hupa, M.; Saviharju, K. Reducing NO<sub>x</sub> emissions using fuel staging, air Staging, and selective noncatalytic reduction in synergy. *Ind. Eng. Chem. Res.* **2005**, *44*, 4552–4561.
42. Ghani, W.A.W.A.K.; Alias, A.B.; Savory, R.M.; Cliffe, K.R. Co-combustion of agricultural residues with coal in a fluidised bed combustor. *Waste Manag.* **2009**, *29*, 767–773.
43. Lin, W.; Jensen, P.A.; Jensen, A.D. Biomass suspension combustion: Effect of two-stage combustion on NO<sub>x</sub> emissions in a laboratory-scale swirl burner. *Energy Fuels* **2009**, *23*, 1398–1405.
44. Houshfar, E.; Løvås, T.; Skreiberg, Ø. Detailed Chemical Kinetics Modeling of NO<sub>x</sub> Reduction in Combined Staged Fuel and Staged Air Combustion of Biomass. In *Proceedings of 18th European Biomass Conference & Exhibition (EU BC&E)*, Lyon, France, 3–7 May 2010; pp. 1128–1132.
45. Baxter, L. Biomass-coal co-combustion: opportunity for affordable renewable energy. *Fuel* **2005**, *84*, 1295–1302.
46. Coda Zabetta, E.; Hupa, M. A detailed kinetic mechanism including methanol and nitrogen pollutants relevant to the gas-phase combustion and pyrolysis of biomass-derived fuels. *Combust. Flame* **2008**, *152*, 14–27.
47. Røjel, H.; Jensen, A.; Glarborg, P.; Dam-Johansen, K. Mixing effects in the selective noncatalytic reduction of NO. *Ind. Eng. Chem. Res.* **2000**, *39*, 3221–3232.
48. Nussbaumer, T. *Biomass Combustion in Europe Overview on Technologies and Regulations*; Report 08-03. Available online: [http://www.nyserda.ny.gov/en/Publications/Research-and-Development/~media/Files/Publications/Research/Biomass%20Solar%20Wind/08-03\\_Biomass-Combustion-in-Europe.ashx](http://www.nyserda.ny.gov/en/Publications/Research-and-Development/~media/Files/Publications/Research/Biomass%20Solar%20Wind/08-03_Biomass-Combustion-in-Europe.ashx) (access on 6 February 2012).

49. Becidan, M.; Houshfar, E.; Khalil, R.A.; Skreiberg, Ø.; Løvås, T.; Sørum, L. Optimal mixtures to reduce the formation of corrosive compounds during straw combustion: A thermodynamic analysis. *Energy Fuels* **2011**, *25*, 3223–3234.
50. Thy, P.; Esbensen, K.H.; Jenkins, B.M. On representative sampling and reliable chemical characterization in thermal biomass conversion studies. *Biomass Bioenergy* **2009**, *33*, 1513–1519.
51. Jiang, X.; Huang, X.; Liu, J.; Han, X. NO<sub>x</sub> Emission of fine- and superfine- pulverized coal combustion in O<sub>2</sub>/CO<sub>2</sub> atmosphere. *Energy Fuels* **2010**, *24*, 6307–6313.
52. Lissianski, V.V.; Zamansky, V.M.; Maly, P.M. Effect of metal-containing additives on NO<sub>x</sub> reduction in combustion and reburning. *Combust. Flame* **2001**, *125*, 1118–1127.

© 2012 by the authors; licensee MDPI, Basel, Switzerland. This article is an open access article distributed under the terms and conditions of the Creative Commons Attribution license (<http://creativecommons.org/licenses/by/3.0/>).